

Transient, High-Pressure Solidification Associated with Cavitation in Water

Robert Hickling

National Center for Physical Acoustics, University of Mississippi, University, Mississippi 38677

(Received 8 September 1994)

The very high pressures (>1 GPa) that occur during the final stages of collapse of a cavitation bubble force the liquid near the bubble wall briefly (~ 1 ns) into a metastable state of subcooling, relative to the equilibrium phase diagram. Estimates for water show that solidification in the form of high-pressure ice particles can occur at a sufficient rate to affect the collapse. This explains a number of different phenomena associated with cavitation in water.

PACS numbers: 47.55.Bx, 43.25+y, 47.40.-x, 78.60.Mq

There has been renewed interest in the physics of cavity collapse or implosion in liquids because recent experimental results [1,2] have determined, for the first time, the surprisingly short duration (<50 ps) of the flashes of light emitted by single cavitation bubbles. Light emission from cavitation, first observed in 1933 [3], is usually called sonoluminescence (SL), because it is detected principally in cavitation induced by sound fields in liquids. The very short duration of SL pulses was discovered following the development of a technique for observing SL from a single, stable bubble [4]. SL is generally believed to be caused by the rapid compression of gas to high temperatures inside collapsing cavitation bubbles, but the details of this mechanism have required further thought, because of the unexpectedly short duration of the SL pulses. This has led to the development of the theory of microshocks converging at the core of the gas in the bubble to create a very short-duration, high-temperature compression [5,6]. It would seem that any explanation of SL and its characteristics has to be consistent with other known effects of cavitation. It is the purpose of this Letter to develop such an explanation based on the assumption of transient high-pressure solidification in the water near the bubble wall during the final stages of bubble collapse.

A characteristic of SL in pure water is that it is enhanced by a factor greater than 10, when the temperature of the water is reduced from about 20 to 5 °C [7], see Fig. 1. SL is also enhanced when the temperature of the water is reduced from 50 to 25 °C [8]. This enhancement with decreasing temperature can be explained assuming transient, high-pressure solidification. The mechanism of transient, high-pressure solidification was first proposed [9] to explain two other effects associated with cavitation, namely, the nucleation of freezing by cavitation in subcooled liquids [10] and the reduction in cavitation erosion as the water temperature approaches 0 °C [11]. The latter effect is exhibited in Fig. 2 for different metals and metal hardnesses, in terms of erosion weight loss as a function of water temperature. In Fig. 2, the reduction in cavitation erosion as the water temperature approaches boiling is due to the increase in vapor pressure inside the bubbles causing a less violent collapse.

The reduction as the water temperature approaches 0 °C is obviously caused by a different mechanism which is hypothesized to be transient, high-pressure solidification. An up-to-date review of available information on the mechanism of cavitation erosion is provided in Ref. [12], which tends to support the shock-wave explanation that is assumed here.

Conditions for transient, high-pressure solidification are created during the final stages of bubble collapse in the water near the bubble wall. Computations have shown that the pressure increase in this region is almost adiabatic attaining values of the order of 5 GPa and higher [9,13]. It has always been believed that very high pressures occur during cavity collapse [12,14], and this is further supported by the recent work on SL. However, that such pressures can force the water into a metastable state of subcooling relative to the equilibrium phase diagram has not been taken into consideration. The nature of the adiabatic increase in pressure and temperature near the bubble wall is indicated in Fig. 3 which shows lines of adiabatic compression, for water initially at atmospheric

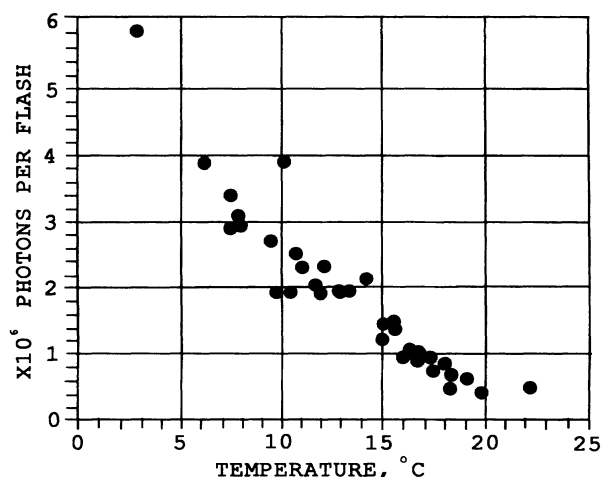


FIG. 1. Number of photons emitted per flash of SL, as a function of water temperature. The output of the brightest bubble was recorded at each temperature. (Reproduced with permission from Ref. [7].)

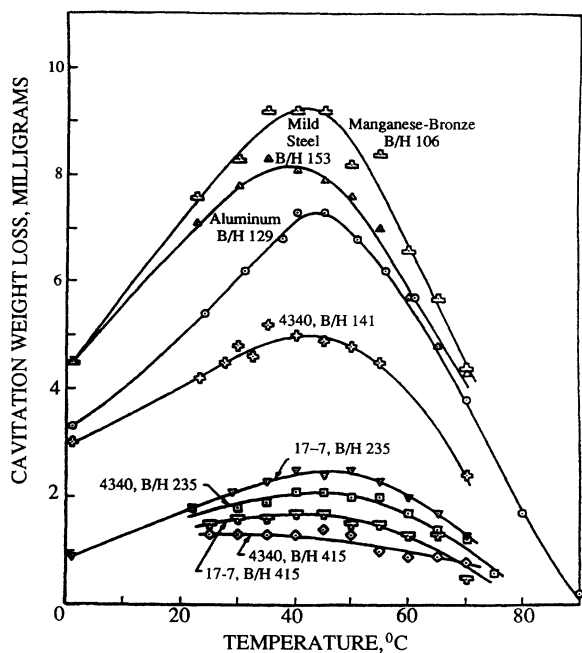


FIG. 2. Weight loss due to cavitation erosion in pure water, as a function of water temperature. Each point represents 15 min of exposure to ultrasonic cavitation, with the vibration of the specimen maintained at constant amplitude. The bottom curves are for different types of steel with different Brinell hardness. The data were taken from Ref. [11].

pressure and at 0, 30, and 60 °C, superimposed on the ice-water equilibrium phase diagram [15]. These were computed using a procedure derived from Ref. [16] based on Bridgman's data for pure water [17] and are extrapolated into the ice phase up to pressures of 4 GPa. These lines provide a conservative estimate of the minimum temperature of subcooling resulting from compression near the bubble wall. For isothermal compression the subcooling would obviously be greater. The 0 °C adiabatic line indicates that there is subcooling of the order of 10^2 K at 4 or 5 GPa. Also for the 0 °C adiabatic line, there is a greater extent of subcooling and more time is spent in the subcooled state than for adiabatic lines originating at higher temperatures. Conditions are right for solidification, if there is enough time. It was shown previously [9] that it is reasonable to assume that (a) subcooling falls below the critical temperature for homogeneous nucleation of freezing, and (b) there is enough time for a growth of ice particles which, because of the greater density of high-pressure ice [18], causes a reduction in pressure next to the bubble wall. If half the water in the high-pressure region next to the bubble wall turns to ice particles, it is estimated that a drop in pressure of about 1 GPa can occur [9]. This will mitigate the forces involved in cavitation erosion, thus causing the decrease in erosion rate shown in Fig. 2, as the water temperature approaches 0 °C. Also, when the water is

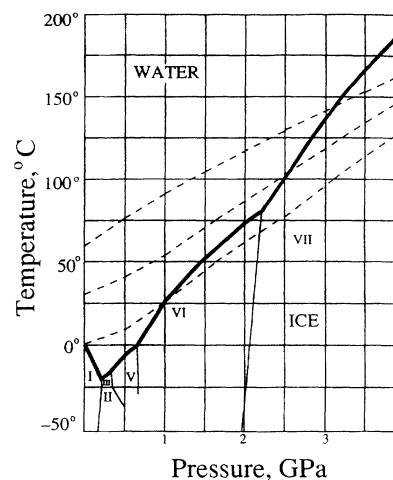


FIG. 3. Computed lines of adiabatic compression (dashed lines) superimposed on the equilibrium ice-water phase diagram. The lines originate in the liquid at atmospheric pressure and at 0, 30, and 60 °C and are extrapolated into the solid phase. These were computed using a method given in Ref. [15]. The Roman numerals in the phase diagram (Ref. [15]) indicate different types of ice.

in an overall subcooled state at atmospheric pressure, solidification associated with cavitation can provide a nucleus for the initiation of freezing.

The very short duration of SL pulses, and the increase in SL intensity with decreasing water temperature shown in Fig. 1, is also explained on the basis of the drop in pressure next to the bubble wall caused by transient, high-pressure solidification. This explanation is linked to the occurrence of converging microshocks in the gas within a collapsing cavitation bubble. The idea that SL is associated with the formation of microshocks is not new [8]. Recent papers [5,6] have provided details of the microshock mechanism. These have shown that very small changes in the conditions of bubble formation and collapse in the acoustic field in the liquid can cause major changes in response, even to the extent of determining whether or not microshocks occur [5]. This uncertainty can be avoided if it is assumed that transient solidification triggers the microshocks. The drop in pressure due to solidification initially causes a rarefaction. However, the compressed water surrounding the solidification zone is moving inward, as shown by computed Mach-number data [13] in Fig. 4, thus creating a converging compression wave following the rarefaction. It is this compression wave converging to the core of the gas in the bubble that causes a high-temperature spike and SL in the gas, accounting for the observed short duration of SL pulses. As the temperature of the water is reduced, the amount, duration, and extent of subcooling is increased, causing an increased amount of solidification, and hence an increased pressure drop, a larger converging compression wave, and a more intense SL pulse, thus

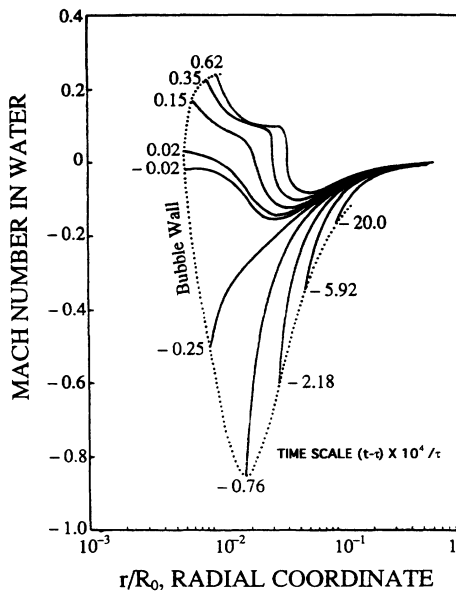


FIG. 4. Variation in Mach number with distance from the bubble wall, at different instants in time during the final stages of collapse and the start of the rebound of a cavitation bubble. Initially the bubble radius is R_0 , the gas pressure is 10 Pa inside the bubble, and the external pressure is 101 kPa in the water. The dotted line in the figure shows the Mach number and the position of the bubble wall and the solid lines are the Mach number distributions along a radius from the bubble wall at different instants in time. Different instants in time are expressed in terms of $(t - \tau)10^4/\tau$ where t is the time variable and τ is the collapse time, from the initial maximum radius R_0 to the minimum radius. Inside the bubble is a uniform adiabatic diatomic gas. It is seen that, when the bubble wall has reached its minimum radius, the Mach number of the water away from the wall is still negative, i.e., moving inward. The data in Fig. 4 were taken from Ref. [13]. They are independent of R_0 .

accounting for the enhancement of SL with decreasing water temperature shown in Fig. 1.

It appears anomalous that bubble collapse can generate a high-temperature spike in the gas inside the bubble, and, at the same time, transient solidification (freezing) in the water next to the bubble wall. Estimates have shown, however, that during the short period of time involved, the amount of heat radiated and conducted from the high-temperature spike does not cause a large enough temperature rise in the water next to the bubble wall to inhibit the solidification [9]. Another apparent anomaly is that cavitation erosion is reduced whereas the intensity of SL pulses is increased, as the water temperature approaches 0 °C. This can be understood by realizing that cavitation erosion is caused by shock waves radiating *outward* from the rebound of the bubble [13], the intensity of these waves being *reduced* in proportion to the amount of solidification near the bubble wall, whereas SL pulses are caused by shock waves converging *inward* [5,6] whose magnitude is *increased* as the amount of solidification increases.

TABLE I. Effect of dissolved gas on intensity of sonoluminescence (Ref. [19]).

Dissolved gas	Relative intensity of sonoluminescence	Thermal conductivity of ($\text{W m}^{-1} \text{K}^{-1}$)
Monatomic		
Helium	1	0.1409
Neon	18	0.0457
Argon	54	0.0161
Krypton	180	0.0089
Xenon	540	0.0052
Diatomic		
Hydrogen	...	0.1733
Oxygen	35	0.0244
Nitrogen	45	0.0230

Another feature of SL in water is the effect of dissolved gas on SL intensity. Dissolved gas diffuses into the cavitation bubbles and affects the SL pulses. As shown in Table I, the range of SL intensity for different gases is quite wide [19]. Calculations have shown that the temperature of the gas compressed inside a collapsing cavitation bubble is significantly affected by heat conduction into the surrounding water [20], the loss of heat occurring principally during the initial slower stages of collapse, prior to the converging microshock that generates SL. But there is also a thermal conduction effect associated with the converging microshock. The thickness or slope of the shock wave is proportional to the thermal diffusivity of the gas [21], and this can cause the variation in SL intensity shown in Table I, because the steeper the converging microshock the more intense the SL pulse. In fact, this may be the predominant cause of the change in SL intensity with different dissolved gases, as was proposed in Ref. [6].

Water is one of only a few liquids whose equilibrium phase diagram has a decrease in the solidification temperature with increase in pressure in the region immediately above atmospheric pressure. If the transient solidification hypothesis is correct, differences between the equilibrium phase diagrams of liquids can be used to explain differences in SL, cavitation erosion, and other effects associated with cavitation in different liquids.

- [1] B.P. Barber and S.J. Putterman, *Nature (London)* **352**, 318–320 (1991).
- [2] B.P. Barber, R. Hiller, K. Arisaka, H. Fetterman, and S.J. Putterman, *J. Acoust. Soc. Am.* **91**, 3061 (1992).
- [3] M. Marinesco, and J.J. Trillat, *Compt. Rend.* **196**, 858–860 (1933).
- [4] D.F. Gaitan, L.A. Crum, C.C. Church, and R.A. Roy, *J. Acoust. Am.* **91**, 3166–3183 (1992).
- [5] C.C. Wu and P.H. Roberts, *Phys. Rev. Lett.* **70**, 3424–3427 (1993).
- [6] H.P. Greenspan and A. Nadim, *Phys. Fluids A5*, 1065–1067 (1993).

- [7] R. Hiller, S.J. Putterman, and B.P. Barber, *Phys. Rev. Lett.* **69**, 1182–1184 (1992).
- [8] P. Jarman, *J. Acoust. Soc. Am.* **32**, 1459 (1960).
- [9] R. Hickling, *Nature (London)* **206**, 915–917 (1965).
- [10] B. Chalmers, *Principles of Solidification* (Wiley, New York, 1964), p. 86.
- [11] R.E. Devine and M.S. Plesset, Division of Engineering, California Institute of Technology Report No. 85-27, 1964.
- [12] C.E. Brennen, *Cavitation and Bubble Dynamics* (Oxford University Press, New York, 1994).
- [13] R. Hickling and M.S. Plesset, *Phys. Fluids* **7**, 7–14 (1964).
- [14] F.R. Young, *Cavitation* (McGraw-Hill, New York, 1989).
- [15] American Institute of Physics Handbook (McGraw-Hill, New York, 1957), p. 4–35.
- [16] J.M. Richardson, A.B. Arons, and R.R. Halverson, *J. Chem. Phys.* **15**, 785–794 (1947).
- [17] J.W. Bridgman, *J. Chem. Phys.* **3**, 597 (1935).
- [18] N.E. Dorsey, *Properties of Ordinary Water Substance* (Reinhold Publishing Corp., New York, 1960), p. 613.
- [19] R.O. Prudhomme and Th. Guilmar, *J. Chim. Phys.* **54**, 336–340 (1957).
- [20] R. Hickling, *J. Acoust. Soc. Am.* **35**, 967–974 (1963).
- [21] H.W. Liepmann and A. Roshko, *Elements of Gas Dynamics* (Wiley, New York, 1957), p. 332.